Processing and Application of Ceramics 13 [2] (2019) 157–163
https://doi.org/10.2298/PAC1902157B

From freeze-dried precursors to microwave sintered Al_2O_3-ZrO_2 composites

Amparo Borrell*, Lorena Gil, René Guillén, María Dolores Salvador

Instituto de Tecnología de Materiales (ITM), Universitat Politècnica de València, Camino de Vera, s/n, 46022 Valencia, Spain

Received 20 November 2018; Received in revised form 3 March 2019; Accepted 15 May 2019

Abstract

Homogeneous Al_2O_3-$Zr_{0.91}Y_{0.09}O_{1.955}$ (65–35 mol%) nanopowders have been prepared in a wide temperature range (from 1073 to 1573 K) by thermal decomposition of amorphous precursors, made previously by freeze-drying of appropriate solutions in air. Electron microscopy images show that, whereas at low temperatures (973 K) pseudo-spherical particles constituted of Al_2O_3 and $Zr_{0.91}Y_{0.09}O_{1.955}$ grains are observed (~38 nm), at high temperatures (1573 K) a homogeneous dispersion of nanocrystalline ZrO_2-based grains (~186 nm) is dispersed in the sintered Al_2O_3 matrix. The comparison between phase and microstructure evolution in these samples clearly indicates that the disorder at the atomic scale in the precursor makes the attainment of higher temperatures necessary for nucleation and growth of both phases. Finally, a selected material was sintered in a mono-mode microwave device at 2.45 GHz in air at 1573 and 1673 K. This fast-microwave technology allows fabrication of composites with high densities (~99% TD) and excellent mechanical properties, such as hardness and Young's modulus reaching 25.6 GPa and 358 GPa, respectively.

Keywords: *ceramic composites, freeze-drying, microwave sintering, microstructure, mechanical properties*

I. Introduction

Alumina and zirconia are two of the most important ceramic materials due to their capability in performing a diversity of applications based on their mechanical, chemical and thermal properties [1,2]. Al_2O_3-ZrO_2 composites also have a prominent engineering role due to their improved mechanical properties compared to Al_2O_3 and ZrO_2 monolithic materials [3]. For example, the flexural strength and fracture toughness of Al_2O_3 can be considerably increased by the incorporation of ZrO_2 particles in an Al_2O_3 matrix (called zirconia-toughened alumina, ZTA) [4]. Previous works demonstrated that improvement in mechanical [5–7], electrical [8,9] and magnetic [10] properties could be achieved by using nanosized powders as raw materials, and by adding dopants to the ceramic matrix. The degree of the improvement is strongly influenced by the organization level and homogeneous distribution of each constituent and depends on size, morphology, purity and extent of the aggregation of the powder primary nanoparticles [11].

* Corresponding authors: tel: +34 963877007,
e-mail: *aborrell@upv.es*

The Al_2O_3-ZrO_2 system usually consists of an alumina matrix in which zirconia particles are dispersed. This composite could be obtained by different methods, such as mechanical mixing, high-energy milling, sol-gel or hydrothermal methods, among others. The development of these methods has opened up wide routes for the improvement of different properties of nanostructured ceramics.

In our previous papers [12,13] we have reported the use of the freeze-drying method in the preparation of different materials. The method consists of fast freezing of a sprayed solution, followed by vacuum drying by sublimation of the solvent. Thus, in this way, it is possible to obtain freeze-dried amorphous precursors. A diversity of nanostructured materials (oxides, nitrides, carbides, intermetallics) has been produced using appropriate thermal treatment in a controlled atmosphere [12–16]. By starting from the solutions of molecular derivatives, the exploration of wide ranges of metal compositions (stoichiometries) is usually feasible in complex systems. Furthermore, sublimation of the solvent results in an intimate mixing of the components in the precursor powders, which decreases the diffusion distances and

generally results in small sized particles after relatively moderate treatments. This method allows the synthesis of polycrystalline powders with controlled characteristics (composition and particle-morphology). In addition, this process can be scaled up for industrial production using currently available equipment, and permits high volumes (appropriate for multigram quantities) and, therefore, satisfactory production rates.

In the present work, the use of the freeze-dried precursors in the preparation of nanopowders containing alumina and zirconia-based components has been investigated. In particular, the composition of Al_2O_3-$Zr_{0.91}Y_{0.09}O_{1.955}$ (65–35 mol%), which has been widely studied for its application as a material of high thermal resistance [17], has been obtained. The influence of the final temperature on the microstructure of the material has been studied. The phase evolution and crystallite sizes of Al_2O_3 and $Zr_{0.91}Y_{0.09}O_{1.955}$ in this composition have been compared with Al_2O_3 or $Zr_{0.91}Y_{0.09}O_{1.955}$ nanopowders obtained with the same precursors separately.

Finally, Al_2O_3-$Zr_{0.91}Y_{0.09}O_{1.955}$ (65–35 mol%) material has been sintered using the non-conventional microwave technique. The microstructure and mechanical properties, such as hardness and Young's modulus, of the Al_2O_3-ZrO_2 nanocomposite are analysed. Microwave sintering technique is a promising method to produce dense materials, that allows to work at heating rates of hundreds of degrees per minute and the energy consumed per test is lower than any current sintering method [18]. These features allow the achievement of microstructures unattainable by other sintering methods and, therefore, obtaining mechanical properties superior to those obtained using a conventional technique [19].

The objective of this work is to demonstrate how the selection of the processing parameters allows the preparation of a homogeneous nanocomposite and, through a non-conventional sintering method, achieve a fully dense alumina-zirconia composite with high mechanical properties for a short fabrication time.

II. Materials and methods

2.1. Synthesis

The materials used as reagents were aluminium L-lactate, $Al(CH_3CHOHCOO)_3$ (Aldrich, 97.0%), zirconium acetate, $Zr(CH_3COO)_4$(Aldrich, solution in dilute acetic acid, 15-16% Zr), yttrium oxide, Y_2O_3 (Aldrich, 99.99%), glacial acetic acid (Panreac, 99.5%) and nitric acid (Panreac, 65.0%).

Preparation of precursors

Y_2O_3 was dissolved under reflux in a solution of acetic acid : ethanol : nitric acid 5 : 1 : 0.02 (v : v : v). By combining this solution with the zirconium acetate reagent solution, we obtained a Zr-Y source solution whose total cationic concentration was 0.60 M, with molar nominal composition Zr : Y = 0.91 : 0.09. On the other hand, an aluminium L-lactate precursor solution (0.60 M of Al^{3+}) was directly prepared by dissolving the salt (0.15 M) in water (250 ml) under continuous stirring at room temperature. By combining the Zr-Y and the Al solutions, we obtained an Al-Zr-Y solution whose total cationic concentration was 0.60 M and with molar nominal composition Al : Zr : Y = 1 : 0.245 : 0.024. The amounts of the different reagents were adjusted to yield 15 g of the final mixture of Al_2O_3 (65 mol%) and $Zr_{0.91}Y_{0.09}O_{1.955}$ (35 mol%), which implies the freeze-drying of approximately 375 ml of the source solution.

Droplets of these solutions were flash frozen by projection on liquid nitrogen and, then, freeze-dried at a pressure of 10^{-4} atm in a Telstar Cryodos freeze drier. In this manner, dried solid precursors were obtained as amorphous, (X-ray diffraction) loose powders. The thermal evolution of the precursors was monitored by thermogravimetric experiments (TGA-DTA) under an oxygen atmosphere (heating rate 5 K/min, flow rate 50 cm^3/min), using a Setaram Setsys 16/18 System.

Synthesis of nanostructured ceramic oxide

The different samples were synthesized by heating the amorphous freeze-dried precursor under air. The precursors (0.5 g) were placed into an alumina crucible of 5 cm^2 of usable surface, and introduced in a tubular furnace. Several experimental conditions were performed in order to determine their influence on the structure and microstructure of the resulting solids. The precursor powders were heated at 5 K/min to a final temperature (T_f = 573 to 1573 K, in steps of 100 K) that was held for a period of time (t_{hold}) of 6 h in air. The solids were then cooled down by turning off the oven leaving the sample inside (slow cooling, 2 K/min). All products were stored in a desiccator over silica gel.

Sintering of Al_2O_3-ZrO_2 by microwave technology

Cylindrical specimens (10 mm diameter, 5 mm height) were prepared by cold isostatic pressing (200 MPa). These specimens were sintered in air via the non-conventional sintering technique of microwave technology. The samples were introduced in a monomode (2.45 GHz) rectangular cavity that is automatically adjusted to optimize microwave absorption and control the heating rate. A variable power output from 0 to 1200 W is possible. In this case, the power has been set to 700 W. In the microwave furnace, the samples were heated without susceptor at 1573 and 1673 K using a heating rate of 200 K/min, and with a holding time at the maximum temperature of 10 min. The temperature of the sample was monitored by an infrared radiation thermometer (Optris CT-Laser LT, 8–14 μm), which was focused on the test sample via the small circular aperture in the wall of the test cell [20].

2.2. Characterization

X-ray powder diffraction (XRD) patterns were obtained from a diffractometer (Brucker AXS-D5005) using Cu-Kα radiation. Samples were dusted through a sieve on the holder surface. Routine patterns were col-

lected with a scanning step of 0.08° in 2θ over the angular range 20–70° with a collection time of 5 s per step. Patterns for microstructural analysis and profile fitting were collected with a scanning step of 0.02° in 2θ over the angular range 20–110° with a collection time of 10 s per step. Profile fittings were performed using the FULLPROF program [21].

The morphology of freeze-dried precursors and the resulting oxide were observed using a scanning field emission electron microscope (FESEM, HITACHI S-4100, Japan) operating at an accelerating voltage of 30 kV. In some cases, the morphology was also observed using a transmission electron microscope (JEOL JEM 1010) operating at 100 kV. In order to analyse the microstructure of the sintered samples, polished sections were thermally etched during 10 min in an electrical furnace under air at 200 K below their maximum sintering temperature. These sections were observed using a field emission scanning electron microscope (FESEM, HITACHI S-4800, Japan) operating at an accelerating voltage of 30 kV. All specimens were covered with a thin film of gold/palladium for better image definition.

The BET surface areas of the products were determined by nitrogen adsorption at 77 K assuming a cross-sectional area of 0.162 nm^2 for the nitrogen molecule, using a Micromeritics ASAP 2000 equipment. Prior to adsorption measurements, the samples were degassed in vacuum at 423 K for 18 h.

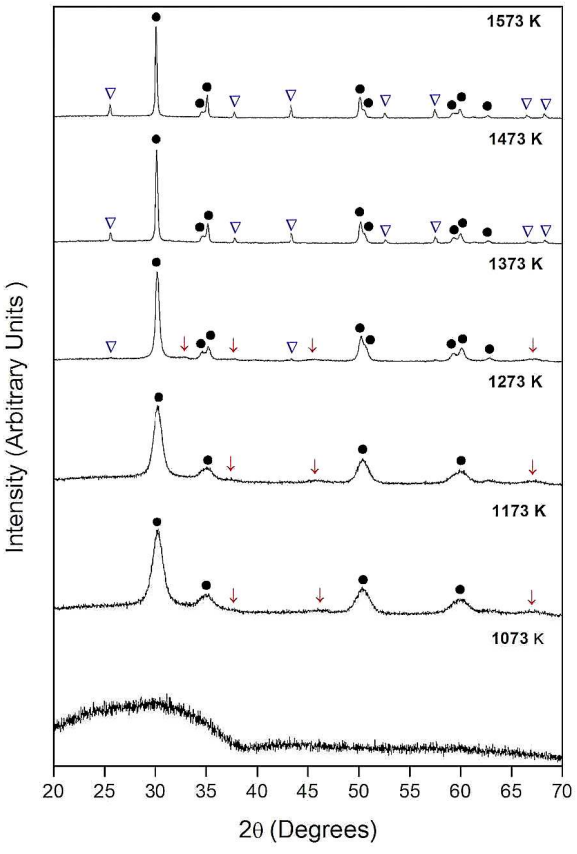

Figure 1. XRD patterns of Al_2O_3-$Zr_{0.91}Y_{0.09}O_{1.955}$ powders (● $Zr_{0.91}Y_{0.09}O_{1.955}$, ▽ α-Al_2O_3, ↓ γ-Al_2O_3)

The bulk density of the samples was measured by the Archimedes method (ASTM C373-88) immersing the sample into a water-based liquid, using theoretical densities of 3.98 and 6.08 g/cm^3 for Al_2O_3 and ZrO_2, respectively. The relative density was calculated by dividing the bulk density by the theoretical density of the powder mixture (4.86 g/cm^3).

Mechanical properties such as hardness and Young's modulus of the samples were obtained by nanoindentation technique (Model G200, MTS Company, USA). The sintered samples were previously cut longitudinally in half cylinders with a diamond saw and polished (Struers, model RotoPol-31) with 0.25 μm diamond paste. To carry out indentations at very low depths, a Berkovich diamond tip was used with radius less than 20 nm. In order to ensure the quality of the tip throughout the test, pre- and post-calibration procedures were performed for this indenter, ensuring the correct calibration of its function area and adequate machine compliance. The mechanical properties of the Al_2O_3-ZrO_2 ceramics were performed under maximum depth control of the 1500 nm. The contact stiffness (S) was determined by continuous stiffness measurement technique to calculate the profiles of hardness (H) and elastic modulus (E). Amplitude was programmed to 2 nm with 45 Hz frequency. A matrix with 26 indentations was performed for each sample [22].

III. Results and discussion

The thermal evolution of the precursor was monitored by means of thermogravimetric analysis (TGA) and X-ray powder diffractometry. The TGA curve shows that decomposition of the precursor yielding oxide is complete at 800 K.

Figure 1 shows the XRD patterns of the powders resulting from the thermal treatment of the Al_2O_3-$Zr_{0.91}Y_{0.09}O_{1.955}$ (65–35 mol%) precursor samples at temperatures ranging from 1073 to 1573 K. The minimum temperature at which crystalline phases were detected (tetragonal modification of ZrO_2 and γ-Al_2O_3) was 1173 K. At 1373 K, the coexistence of γ-Al_2O_3 and α-Al_2O_3, together with tetragonal ZrO_2, was observed. Finally, at 1473 and 1573 K, only tetragonal ZrO_2 and α-Al_2O_3 were detected. JCPDS patterns of tetragonal ZrO_2 (81-1546), α-Al_2O_3 (71-1123) and γ-Al_2O_3 (10-0425) match with the observed XRD.

Figure 2 shows a scheme of the phases observed in these experiments compared with other experiences in which the equivalent Al_2O_3 and $Zr_{0.91}Y_{0.09}O_{1.955}$ precursors were exposed to the same thermal treatments. In the thermal decomposition of a precursor obtained by freeze-drying of aluminium lactate solution, the first crystalline phase observed was γ-Al_2O_3 at 1173 K. At 1373 K, both γ- and α-Al_2O_3 coexists. Finally, between 1473 and 1573 K, only α-Al_2O_3 was detected. On the other hand, in the thermal decomposition of a precursor obtained by freeze-drying of Zr : Y = 0.91 : 0.09

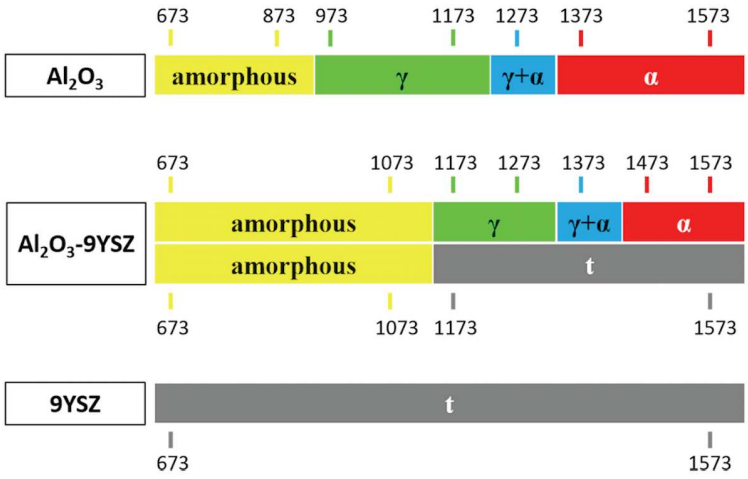

Figure 2. Existence fields of the different phases present in materials prepared by thermal decomposition in oxygen of the Al_2O_3, Al_2O_3-$Zr_{0.91}Y_{0.09}O_{1.955}$ (65–35 mol%) and $Zr_{0.91}Y_{0.09}O_{1.955}$ precursors

acetic acid solution, tetragonal ZrO_2 was detected between 673 and 1573 K.

As a consequence, the presence of Al_2O_3 (65 mol%) inhibits the crystallization of tetragonal zirconia up to 1173 K. On the other hand, the presence of $Zr_{0.91}Y_{0.09}O_{1.955}$ (35 mol%) causes delay of the γ-Al_2O_3 crystallization for 200 K, and α-Al_2O_3 crystallization for 100 K.

Selected microstructural data for Al_2O_3-$Zr_{0.91}Y_{0.09}O_{1.955}$ nanopowders prepared at different temperatures (973, 1173, 1373 and 1573 K) are summarized in Table 1. The crystallite sizes, estimated using the Debye-Scherrer equation (d_{DRX}), have been obtained for $Zr_{0.91}Y_{0.09}O_{1.955}$ by analysis of the 101 tetragonal reflection (the intensities of the α-Al_2O_3 reflections are very low, which precludes the realization of a similar analysis for this phase). Crystallite size is approximately 5 nm at 1173 K. The growth with temperature reaches 47 nm at 1573 K. For comparison with the decomposition of the equivalent Zr precursor at 1173 K, the crystallite size was 18 nm, and grows up to 55 nm at 1573 K.

The particle size is obtained from scanning electron microscope images (d_{SEM}); specific surface area (S_{exp}) is calculated assuming non-aggregated particles with sizes obtained from SEM images (S_{calc}).

Both results, the delay in the crystallization of Al_2O_3 (α- and γ- phases) and $Zr_{0.91}Y_{0.09}O_{1.955}$ and the small crystallite size, suggest that the nucleation and growth require higher temperatures to occur due to the atomic disorder in the nanocomposite precursor at the atomic scale compared with the pure Al and Zr cases.

Figure 3 shows characteristic FE-SEM and TEM images corresponding to Al_2O_3-$Zr_{0.91}Y_{0.09}O_{1.955}$ nanopowders obtained at 973, 1373 and 1573 K. The sample prepared at 973 K constitutes of aggregates of pseudo-spherical (~38 nm) particles (Fig. 3a,b). At this temperature, crystallites have not grown sufficiently to diffract. At 1373 K the images show a similar microstructure, with particle size around 50 nm (Fig. 3c,d). At 1573 K the sample constitutes of relatively small particles (~186 nm) dispersed in a sintered matrix (Fig. 3e). The TEM images (Fig. 3f) show that the

Table 1. Microstructural data for Al_2O_3-$Zr_{0.91}Y_{0.09}O_{1.955}$ nanopowders prepared at different temperatures

	973 K	1173 K	1373 K	1573 K
d_{DRX} [nm]	-	5	16	47
d_{SEM} [nm]	38	42	57	186*
S_{calc} [m^2/g]	35	31	23	-
S_{exp} [m^2/g]	2.7	1.9	1.7	1

* $Zr_{0.91}Y_{0.09}O_{1.955}$ particle size

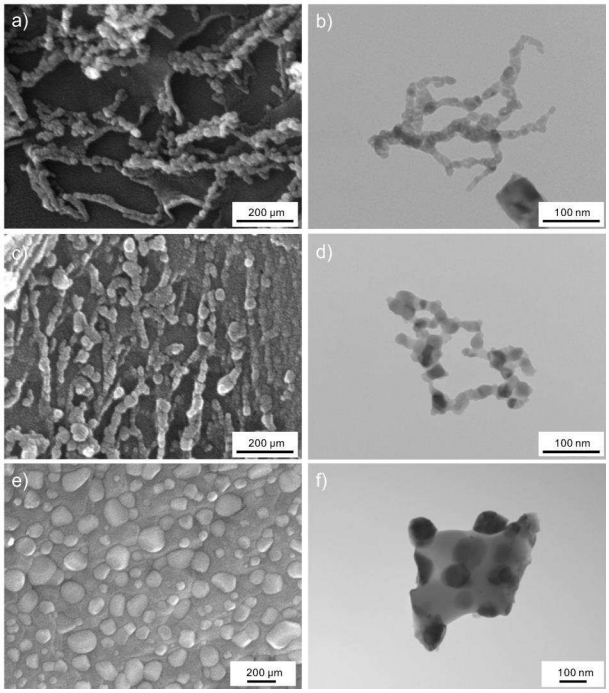

Figure 3. Scanning and transmission electron microscope images showing the microstructure of Al_2O_3-$Zr_{0.91}Y_{0.09}O_{1.955}$ nanopowders heated at: 973 K (a,b), 1373 K (c,d) and 1573 K (e,f)

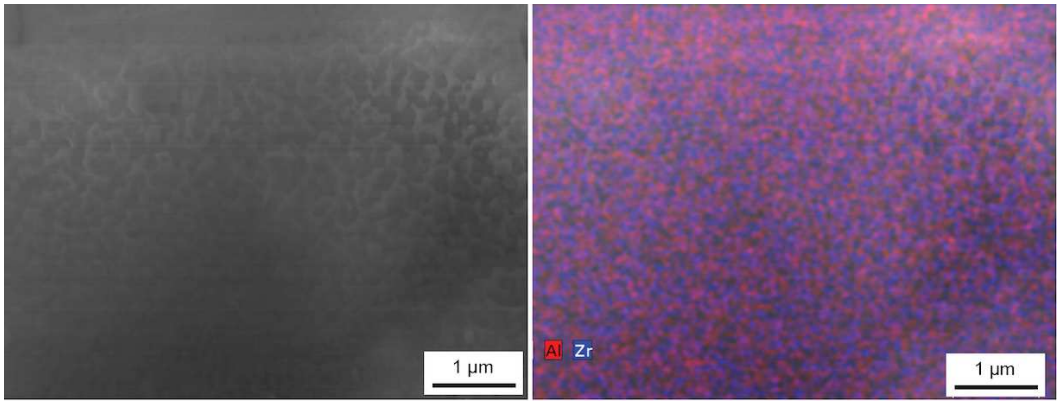

Figure 4. FE-SEM image (a) and compositional map (b) of – $Zr_{0.91}Y_{0.09}O_{1.955}$ (65–35 mol%) prepared from a freeze-dried precursor at 1573 K

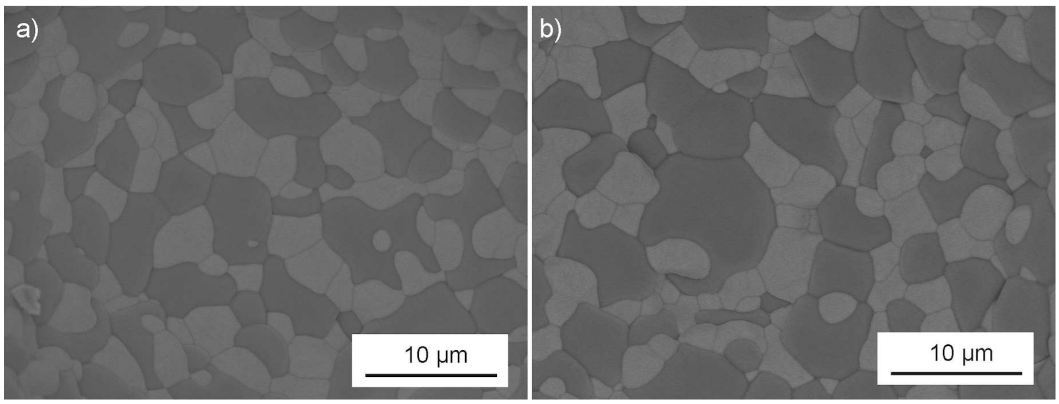

Figure 5. FE-SEM micrographs of nearly full dense Al_2O_3-ZrO_2 composites obtained by microwave sintering at: a) 1573 K and b) 1673 K

small particle absorbs more electrons than the matrix. In consequence, the samples contain relatively small particles of $Zr_{0.91}Y_{0.09}O_{1.955}$ dispersed in an Al_2O_3 matrix.

Finally, Figure 4 shows a compositional mapping of Al and Zr in the Al_2O_3-$Zr_{0.91}Y_{0.09}O_{1.955}$ sample prepared at 1573 K. As can be observed, a homogeneous distribution of Zr and Al exists in the sample, indicating uniform distribution of $Zr_{0.91}Y_{0.09}O_{1.955}$ particles in the Al_2O_3 matrix.

The temperature induced microstructural evolution is clearly reflected in the variation of the measured BET surface areas (S_{exp}) of the solids (see Table 1). The S_{exp} values are significantly lower than what could be expected from the experimental (SEM) particle sizes (i.e. surface approximate values than can be estimated assuming spherical particles, S_{calc}). A strong particle aggregation in the powder samples exists, which implies that a significant part of the surface of the particles is inaccessible for BET measurements (interface between particles or closed pores).

Table 2 summarizes the sintering conditions and the mechanical properties (hardness and Young's modulus) obtained for the Al_2O_3-ZrO_2 composites sintered by the microwave technique. Fully dense composites were obtained at the selected temperatures with a dwell time of 10 min at the maximum temperature. Density values were close to theoretical values.

The FE-SEM micrographs of the alumina-zirconia ceramics prepared by microwave sintering are shown in Fig. 5. As it can be seen, the zirconia grains were homogeneously dispersed in the alumina matrix (Al_2O_3 - dark grains and ZrO_2 - light grains). There is a clear difference in grain size between the sample sintered at 1573 K with respect to the one obtained at 1673 K. At the higher temperature, the average grain size of Al_2O_3 and ZrO_2 is twice that of the sample at 1573 K. This microstructure has a significant influence on the mechanical properties.

A remarkable fact is that fully dense material with excellent mechanical properties can be obtained by microwave sintering at a lower temperature (1573 K). The hardness and Young's modulus decrease with the in-

Table 2. Hardness and Young's modulus values of the composites sintered by the microwave technique

Sintering temperature [K]	Density [% TD]	Hardness [GPa]	Young's modulus [GPa]
1573	99.1 ± 0.05	25.6 ± 2.1	358 ± 10.1
1673	99.4 ± 0.05	23.1 ± 2.3	305 ± 11.3

crease in the sintering temperature. Mechanical properties appeared highly dependent on the sintering conditions. A Young's modulus of 358 GPa and hardness of 25.6 GPa measured on the Al_2O_3-ZrO_2 composite sintered at 1573 K allow the use of this material in some structural applications. The mechanical values increase due to the small particle growth during microwave sintering.

IV. Conclusions

In summary, homogeneous Al_2O_3-$Zr_{0.91}Y_{0.09}O_{1.955}$ (65–35 mol%) nanopowders have been successfully prepared by thermal decomposition of precursors previously obtained by freeze-drying of the appropriate solutions. The atomic disorder in the precursor determines the evolution of phases, in which case crystallisation starts at higher temperatures than in the monophasic precursor. This influence is also seen with the grain (crystallite) sizes of $Zr_{0.91}Y_{0.09}O_{1.955}$, which are lower than that of the monophasic case. It is also essential to obtain the homogeneous dispersion of $Zr_{0.91}Y_{0.09}O_{1.955}$ nanoparticles.

Sintering behaviour of the Al_2O_3-ZrO_2 nanopowder compacts is studied in the present work using non-conventional microwave fast sintering. Due to the positive effect of microwaves on the densification, Al_2O_3-ZrO_2 materials showed a high-density value at relatively low temperature (1573 K) and excellent mechanical properties. Concerning microstructure changes, our results show a homogeneous distribution of ceramic grains. Also, the grain size was dependent on the maximum sintering temperature achieved. Such results are the consequence of two factors. The first is the initial homogeneous distribution of Al_2O_3 and ZrO_2 nanoparticles attained using precursors obtained by freeze-drying. The second factor is the use of microwave technology to sinter this composite, which allows a full densification. Although the particle size in the sintered pieces is micrometric, the homogeneous distribution of ZrO_2-based particles and the full densification provides superior mechanical properties. Finally, the observed dependence of mechanical properties on particle size opens the way to improve the mechanical properties of the final sintered pieces by controlling the sintering parameters. Such work is in progress.

Acknowledgement: The authors would like to thank to the Generalitat Valenciana for financial support received for the project PROMETEU/2016/040 and Santiago Grisolía program scholarship (GRISOLIAP/2018/168). A. Borrell acknowledges the Spanish Ministry of Economy and Competitiveness for her RyC contract (RYC-2016-20915).

References

1. A.Z.A. Azhar, M.M. Ratnam, Z.A. Ahmad, "Effect of Al_2O_3/YSZ microstructures on wear and mechanical properties of cutting inserts", *J. Alloys Compd.*, **478** (2009) 608–614.
2. Y.P. Ye, J.G. Li, H.D. Zhou, J.M. Chen, "Microstructure and mechanical properties of yttria-stabilized ZrO_2/Al_2O_3 nanocomposite ceramics", *Ceram. Int.*, **34** (2008) 1797–1803.
3. C. Dupas, P. Houdy, M. Lahmani, *Nanoscience: Nanotechnologies and Nanophysics*, Springer, Berlin, 2007.
4. J. Wang, R. Stevens, "Review zirconia-toughened alumina (ZTA) ceramics", *J. Mater. Sci.*, **24** [10] (1989) 3421–3440.
5. K. Niihara, "New design concept of structural ceramics", *J. Ceram. Soc. Japan*, **99** (1991) 974–982.
6. R. Benavente, M.D. Salvador, F.L. Penaranda-Foix, E. Pallone, A. Borrell, "Mechanical properties and microstructural evolution of alumina-zirconia nanocomposites by microwave sintering", *Ceram. Int.*, **40** (2014) 11291–11297.
7. A. Sawaguchi, K. Toda, K. Niihara, "Mechanical and electrical properties of silicon nitride-silicon carbide nanocomposites material", *J. Am. Ceram. Soc.*, **74** (1991) 1142–1144.
8. H.J. Hwang, M. Toriyama, T. Sekino, K. Niihara, "In Situ fabrication of ceramic/metal nanocomposites by reduction reaction in barium titanate/metal oxides systems", *J. Eur. Ceram. Soc.*, **18** (1998) 2193–2199.
9. H. Hyuga, Y. Hayashia, T. Sekinoa, K. Niihara, "Fabrication process and electrical properties of $BaTiO_3$/Ni nanocomposites", *Nanostruct. Mater.*, **9** (1997) 547–550.
10. L.C. De Jonghe, "Ceramic processing for magnetic applications", *Mater. Sci. Eng. B*, **3** (1989) 427–429.
11. X. Feng, M.Z. Hu, "Ceramic nanoparticles synthesis", pp. 687–726 in *Encyclopedia of Nanoscience and Nanotechnology*, Vol. 8. Ed. H.S. Nalwa, American Scinetific Publishers, USA, 2004.
12. R. Villanueva, A. Gómez, P. Burguete, E. Martínez, A. Beltrán, F. Sapiña, M. Vicent, E. Sánchez, "Nanostructured alumina from freeze-dried precursors", *J. Am. Ceram. Soc.*, **94** (2011) 236–243.
13. A. Gómez, R. Villanueva, D. Vie, S. Murcia-Mascaros, E. Martínez, A. Beltrán, F. Sapiña, M. Vicent, E. Sánchez, "Large scale synthesis of nanostructured zirconia-based compounds from freeze-dried precursors", *J. Solid Stat. Chem.*, **197** (2013) 120–127.
14. S. Alconchel, F. Sapiña, D. Beltrán, A. Beltrán, "A new approach to the synthesis of molybdenum bimetallic nitrides and oxynitrides", *J. Mater. Chem.*, **9** (1999) 749–755.
15. P. Burguete, E. Martínez-Tamayo, F. Sapiña, V. Bonache, M.D. Salvador, E. Sanchez, "Synthesis and processing of nanocrystalline tungsten carbide: Towards cemented carbides with optimal mechanical properties", *Int. J. Ref. Met. Hard Mater.*, **29** (2011) 78–84.
16. D. Vie, N. Valero, E. Martínez, F. Sapiña, J.V. Folgado, A. Beltrán, "A new approach to the synthesis of intermetallic compounds: mild synthesis of submicrometric Co_xM_y (M = Mo, W; x : y = 3 : 1 and 7 : 6) particles by direct reduction of freeze-dried precursors", *J. Mater. Chem.*, **12** (2002) 1017–1021.
17. N.H. Menzler, F. Tietz, S. Uhlenbruck, H.P. Buchkremer, D. Stöver, "Materials and manufacturing technologies for solid oxide fuel cells", *J. Mater. Sci.*, **45** (2010) 3109–3135.
18. A. Borrell, M.D. Salvador, F.L. Peñaranda-Foix, J.M. Catala-Civera, "Microwave sintering of zirconia materials:

Mechanical and microstructural properties", *Int. J. Appl. Ceram. Technol.*, **10** [2] (2013) 313–320.
19. M. Oghbaei, O. Mirzaee, "Microwave versus conventional sintering: A review of fundamentals, advantages and applications", *J. Alloys Compd.*, **494** (2010) 175–189.
20. A. Borrell, M.D. Salvador, M. Miranda, F.L. Peñaranda-Foix, J.M. Cátala-Civera, "Microwave technique: A powerful tool for sintering ceramic materials", *Curr. Nanosci.*, **10** (2014) 32–35.
21. J. Rodriguez-Carvajal, "FullProf program", pp. 127–128 in *Collected Abstracts of Powder Diffraction Meeting*, Tolousse, France, 1990.
22. W.C. Oliver, G.M. Pharr, "An improved technique for determining hardness and elastic modulus using load and displacement sensing indentation experiments", *J. Mater. Res.*, **7** (1992) 1564–1583.